Sampling-time harmonic control for cascaded h-bridge converters with thermal control

Marquez, A., Monopoli, V.G., Leon, J.I., Ko, Y., Buticchi, G., Vazquez, S., Liserre, M., Franquelo, L.G.

University of Nottingham Ningbo China, 199 Taikang East Road, Ningbo, 315100, Zhejiang, China.

First published 2020

University of Nottingham
UK | CHINA | MALAYSIA

Sampling-Time Harmonic Control for Cascaded H-Bridge Converters with Thermal Control

Abraham Marquez, *Member*, *IEEE*, Vito Giuseppe Monopoli,*Senior Member*, *IEEE*, Jose I. Leon, *Fellow Member*, *IEEE*, Youngjong Ko, *Student Member*, *IEEE*, Giampaolo Buticchi, *Senior Member*, *IEEE*, Sergio Vazquez, *Senior Member*, *IEEE*, Marco Liserre, *Fellow Member*, *IEEE*.
and Leopoldo G. Franquelo, *Fellow Member*, *IEEE*.

***Index Terms*—Harmonic analysis, Pulse width modulation, Multilevel converters.**

***Abstract*—Cascaded H-bridge converter (CHB) is a multilevel topology that is a well-suited solution for multiple applications such as flexible ac transmission systems or motor drives. This paper is focused on a CHB where the cells present an aging mismatch. This can be caused by the maintenance operation which forces to replace some damaged cells of the converter with new or repaired ones. In this paper, a new improved approach of the active thermal control (ATC) of the CHB using Discontinuous PWM (D-PWM) is presented. The D-PWM technique is used to reduce the power losses of one cell reducing its average temperature in order to increase its remaining lifetime. However, the combination of D-PWM with traditional Phase-Shifted PWM (PS-PWM) introduces high harmonic distortion in the output voltage of the CHB converter at twice the carrier frequency. A detailed harmonic distortion analysis of the CHB output voltage when the D-PWM based ATC is active is presented. From this analysis, a modification of the traditional PS-PWM is derived to eliminate the harmonic distortion at twice the carrier frequency. Experimental results show how the ATC using D-PWM is achieved whereas the harmonic distortion around twice the carrier frequency is eliminated.**

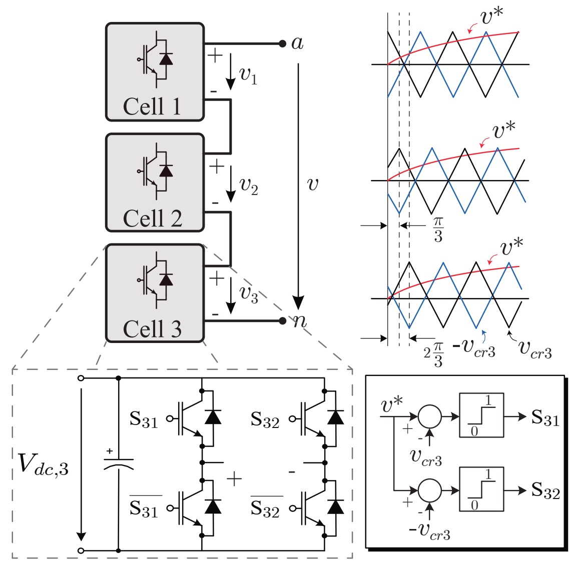

Fig. 1: Three-cell multilevel cascaded H-bridge converter (CHB): Topology and conventional PS-PWM modulation technique

I. Introduction

Nowadays, multilevel converter is a mature technology which has been developed since decades [1]. Multilevel converters are used in a extended range of power applications like pumps, fans, power quality applications and also in renewable energy integration [2], [3]. Among this family, a popular multilevel topology is the cascaded H-bridge converter (CHB) which is shown in Fig. 1 and particularized for a three-cell CHB. This topology was proposed for first time in the early 70's by McMurray [4]. CHB is composed by the series connection of several H-bridges as shown in Fig. 1. Traditionally, the basic power cell is the H-bridge, however it is possible to find in the literature other power cells like NPC or T-type [5]. Among other advantages, this topology is very popular because is able to achieve very high nominal output voltages with a large number of voltage levels providing a high modularity and natural fault-tolerant capability. This fact makes the CHB converter a good candidate to build the Smart Transformer (ST) [6], [7]. The high quality of the output voltage and current makes the CHB one of the most used topologies for medium and high-voltage applications [8].

There are many modulation techniques to operate a CHB converter in the literature, from optimized pulses like selective harmonic mitigation [9] to modulation methods based on multi-carriers [10]. In fact, CHB has most frequently been

Manuscript received Sep 20, 2018; revised Dec 31, 2018 and Feb 01, 2019; accepted March 13, 2019.

The authors gratefully acknowledge financial support provided by the Spanish Science and Innovation Ministry under project TEC2016-78430-R. Section II was made possible by NPRP 9-310-2-134 from the Qatar National Research Fund (a member of Qatar Foundation). The statements made herein are solely the responsibility of the authors.

V. G. Monopoli is with the Department of Electrical and Information Engineering, Politecnico di Bari, 70126 Bari, Italy (e-mail: vitogiuseppe.monopoli@poliba.it).

A. Marquez, J. I. Leon, S. Vazquez and L. G. Franquelo are with the Electronic Engineering Department, Universidad de Sevilla, Seville, 41092 Spain (e-mail: amarquez@ieee.org). L. G. Franquelo is also with the School of Astronautics, Harbin Institute of Technology, Harbin 150001, P. R. China (e-mail: lgfranquelo@ieee.org).

Y. Ko and M. Liserre are with the Chair of Power Electronics, Christian-Albrechts-University of Kiel, Kiel 24143, Germany (e-mail: yoko@tf.uni-kiel.de; ma@tf.uni-kiel.de; ml@tf.uni-kiel.de).

G. Buticchi is with the University of Nottingham Ningbo China, Ningbo 315100, China (e-mail: giampaolo.buticchi@nottingham.edu.cn).

operated using the well-known phase-shifted PWM (PS-PWM) technique. Each power cell is operated using a conventional unipolar PWM technique applying triangular carriers with frequency f_c. In order to implement the PS-PWM method, it is necessary to apply a phase displacement between triangular carriers of consecutive power cells. This phase displacement is usually defined as an angle which is equal to $180°$ (π radians) divided by the number of cells available in each phase, denoted by M [11]. In order to illustrate this idea, the PS-PWM concept as well as the unipolar modulation technique are represented in Fig. 1.

As it is well-known, PS-PWM method presents some advantages when it is applied to a CHB converter. As an example, the output voltage presents high equivalent switching frequency because of the PS-PWM multiplicative effect. Therefore, assuming a switching frequency of each power cell equal to f_c, the CHB output voltage features a harmonic behavior that is equivalent to that produced by a converter with a switching frequency equal to $2Mf_c$. In addition, it also provides a power equalization between modules [12] because the voltage references are equal for all cells. Therefore, a natural equal distribution of power losses, temperature and aging is achieved. PS-PWM operation for a CHB is shown in Fig. 2 for two complete periods until $t = 40ms$ with 150 volts as dc capacitor voltages and a modulation index equal to 0.8.

Power converter failure is mainly caused by the cumulative aging of power devices which is proportional to the thermal stress they suffer during the converter operation. Thermal stress leads to a fatigue of the materials of which the semiconductors are composed. In other words, the reiteration of thermal cycles leads to the expansion and compression of materials which increases the thermal resistance becoming in a non-stop cycle [13]–[15]. This point is well-known in the academia and industry which are focusing their efforts to develop predictive models to obtain the expected remaining power devices lifetime as a function of the suffered thermal cycles [16], [17].

Fault-tolerant capability for CHB allows its operation even if a power cell fault occurs, that means, the maintenance operation is straight-forward because the cells responsible of the fault can be bypassed. In this way, the power converter is able to continue its operation whereas the damaged cells are repaired or substituted by new ones [18]. Consequently, the maintenance operations lead to an aging mismatch among the power cells. That means, the substituted power cells present a different cumulated aging compared with the others, and therefore, after a long-term operation, a non-negligible damage mismatch can be found among the cells [19].

II. Overview of Active Thermal Control for CHB Converters

Active Thermal Control (ATC) is a control strategy which allows the modification of the thermal stress suffered by the modules taking an action over the electrical parameters [15]. Power devices lifetime model estimates the remaining lifetime as a function of cumulated damage which depends on the thermal cycles suffered. The power device damage is estimated taking into account the number of thermal cycles and their deepness. The damage is strongly influenced by the actual power devices temperature, causing more damage with increasing temperature [20]. In this way, the ATC modifies the operation of each module managing the power losses and therefore, making possible to decrease the power devices average temperature reducing the impact of future thermal cycles [21].

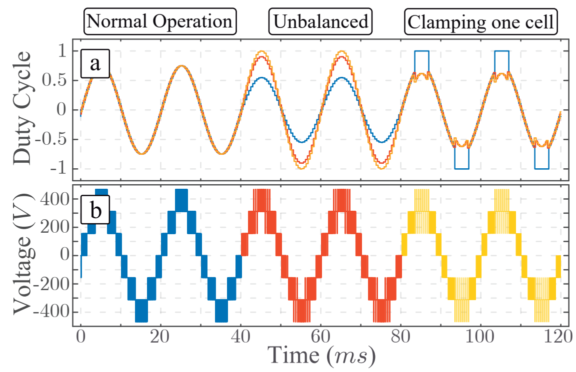

Fig. 2: Active thermal control strategies. a) Duty Cycle b) Output voltage

To develop an effective ATC method for the CHB, two complementary methods can be considered. One possible technique to manage the aging mismatch between modules is to apply a different modulation index to each power cell. In this way, the more damaged cell would produce less voltage than others at its output terminals. As consequence, as the same current flows between all the power modules, each cell manages a different power level. The aged cells will operate with a reduced modulation index whereas the less aged cells compensate this operation mismatch increasing their modulation indexes [22]. This technique is shown in Fig. 2a from 40 to $80ms$ where the first cell is controlled to have a 30% of reduction in its processed power.

As an alternative, it is possible to deal with the switching losses generated in each power cell using the discontinuous PWM (D-PWM) technique. In other words, it is possible to force the generation of the maximum voltage available in the cell during a part of grid-period, avoiding hence the associated switching losses [23]. Therefore, to maintain the desired operation point, the remaining cells must compensate the voltage excess decreasing their reference voltages. This approach has been also represented in Fig. 2a from 80 to $120ms$ using a clamping angle equal to $60°$.

Both methods (modifying the modulation index [22] and clamping one cell [23]) can be applied in order to desing an ATC for the CHB. This means that both methods can manage the temperature of the CHB power devices according to their remaining lifetime. In addition, it can be noticed that both methods are complementary and can be applied simultaneously if it is required. This paper is mainly focused on the study of the ATC method based on clamping one cell in the CHB.

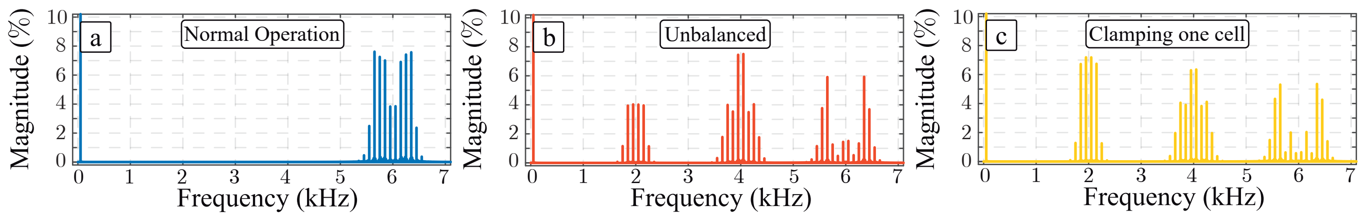

Fig. 3: Output voltage spectrum. a) PS-PWM b) Unbalanced operation c) D-PWM

However, it is important to notice that, when the ATC takes control over the electrical magnitudes, the CHB output voltage is deteriorated increasing its total harmonic distortion (THD) value. It is easy to see that the ATC application leads to an unequal power distribution between the cells and therefore, the natural advantages of PS-PWM technique are partially lost. This phenomenon can be observed taking into account the harmonic spectrum of the CHB output voltage. When the ATC is active forcing an unbalanced operation (different modulation indexes or applying D-PWM), a high harmonic distortion appears located at $2f_c$. This fact is possible to be observed in Fig. 3b and Fig. 3c drawn in red and yellow, respectively considering f_c equal to $1\ kHz$ [24]. The main impact of this low-order harmonic distortion is related to the output filter of the CHB, which has to be designed to keep the output waveforms quality above the minimum standards. If a harmonic distortion at $2f_c$ appears, the required output filter is more expensive, heavy and bulky. In this way, operating properly the CHB this harmonic distortion can be reduced and the output filter is improved in terms of economical cost, weight and size.

This undesirable phenomenon has been studied by the academia in past years leading to the development of some recent modulation techniques. Some of them are based on the feed-forward idea according with real dc voltages present in the converter to carry out some calculations in order to determine the needed duty cycles. As an example, this strategy has been developed in [25], [26] for PS-PWM and [27]–[29] for space-vector modulation techniques. However, none of these proposals deal with the harmonic distortion generated at $2f_c$.

Focusing on harmonic distortion located at twice the carrier frequency, different solutions have been proposed in the literature. For instance, in [30] the conventional PS-PWM technique is modified to reduce the low harmonic content when dc voltages are unequal. This method has been further investigated in [31], [32]. Finally, using the Fourier analysis, in [33] a technique considering the harmonic detail of the pulses generated by PS-PWM is developed. In this way, the method introduced in [33] allows the harmonic cancellation considering different dc voltages and modulation indexes. This is done performing, every sampling time, the analysis of all the H-bridge pulses.

In this paper, a new approach of the ATC using D-PWM for one H-bridge of the CHB is presented. The proposed method is based on the calculation of the displacements angles between carriers in the PS-PWM method each sampling time. The proposed method is able to eliminate the harmonic distortion located at $2f_c$ under an unbalanced operation of CHB.

It is important to highlight that the ATC based on clamped cells in the CHB is not a contribution of this paper. As commented previously, this idea was presented in [23] clearly demonstrating the good performance of the method from the temperature management point of view. Taking this fact into account, the proposed paper uses the ATC method presented in [23] but modifying its final implementation by changing the modulation strategy of the cells. As the obtained CHB output voltages and currents using the proposed method are very similar (differences are negligible) to those obtained in [23], we can extract the same conclusions using the proposed method than those presented in [23] about the thermal behavior of the clamping cells method. The main contribution of the proposed method compared with [23] is the improvement in the harmonic response because the harmonic distortion at low frequency is eliminated. Furthermore, the proposed method can be compared with that proposed in [34] where the phase displacement angles in the PS-PWM method are obtained by complex calculations every fundamental period. In [34], it can be observed that the ATC is achieved successfully using the clamping-cell method as expected. The idea introduced in [34] helps to eliminate the distortion specifically located at twice the carrier frequency but it ignores the sidebands of that group of harmonics. In the proposed method, as the phase displacement angles are determined every sampling period, that harmonics group is completely eliminated improving [34] results.

III. Sampling-Time Harmonic Analysis of the CHB Output Voltage Using PS-PWM

In the CHB operation, the voltage generated by each power cell can be interpreted and modeled as a square pulse train which depends on a variable duty cycle D. This concept is clearly shown in Fig. 4 where the output voltage generated by a single power cell is plotted (in blue) using an conventional unipolar modulation technique. It is also possible to observe the voltage reference drawn in red. A detail of this waveform is presented in Fig. 4 highlighting a single period T_c.

The output voltage waveform of the k-th power cell of the CHB depends on a variable duty cycle which is defined as the ratio between the output voltage reference proposed by the control scheme (v_k^*) and the dc voltage ($V_{dc,k}$):

$$D_k = \frac{v_k^*}{V_{dc,k}}, \text{ where } D_k \in [-1, 1] \tag{1}$$

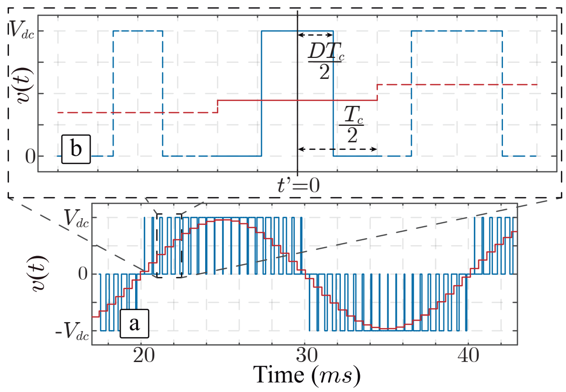

Fig. 4: Output voltage of an H-bridge applying a unipolar PWM method. a) A complete period b) A detail

In order to study the spectral components of the k-th H-Bridge output voltage $v_k(t)$, it is analyzed using the Fourier expansion series. This mathematical tool asserts that, under mild assumptions, a periodic signal can be expressed as a dc component plus an infinite sum of sine and cosine products as follows:

$$v_k(t) = \frac{a_{0k}}{2} + \sum_{n=1}^{\infty} \Big[a_{nk} \cos(n\omega t) + b_{nk} \sin(n\omega t) \Big] \tag{2}$$

where $\omega = {}^{2\pi}/_{(T_c/2)}$ because $2f_c$ is considered the fundamental frequency in the analysis.

Focusing on Fig. 4b and choosing the time origin smartly on t', $v_k(t)$ presents an even symmetry. This is significantly advantageous because the coefficients calculation is simplified due to b_{nk} term is zero. Therefore, it is only required to calculate the a_{nk} coefficients as follows:

$$\begin{aligned} a_{nk} &= \frac{1}{T_c} \int_{\frac{-T_c}{2}}^{\frac{T_c}{2}} v_k(t) \cos(n\omega t) dt \\ &= \frac{2}{T_c} \int_{0}^{\frac{DT_c}{2}} V_{dc,k} \cos(n\omega t) dt \\ &= \frac{2V_{dc,k}}{n\pi} \left[\sin\left(\frac{2\pi n}{T_c} t \right) \right] \Bigg|_0^{\frac{D_k T_c}{2}} \\ &= \frac{2V_{dc,k}}{n\pi} \sin(n\pi D_k) \end{aligned} \tag{3}$$

In Fig. 5, it is represented a comparison between the output voltage of an H-bridge and its Fourier expansion series using the previous calculations (up to 20-th harmonic content). The Fourier expansion series matches with the pulse train being the only difference between both signals the peaks due to the Gibbs effect [35].

So, using the Fourier coefficients, the output voltage of k-th H-bridge can be expressed as:

$$v_k(t) = V_{dc,k} D_k + \sum_{n=1}^{\infty} \Big[\frac{2V_{dc,k}}{n\pi} \sin(n\pi D_k) \cos(n\omega t) \Big] \tag{4}$$

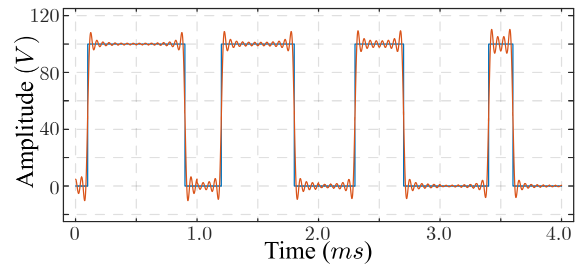

Fig. 5: Output voltage of an H-bridge and the waveform obtained with its Fourier expansion series expression considering harmonics up to $n = 20$-th

All power modules have the same voltage expression and the difference between their output voltages in a CHB is related to the phase displacement present in the PS-PWM method. Conventionally, for a CHB with M-cells per phase operating with PS-PWM and using an unipolar PWM per cell, the phase displacement of k-th power cell is defined by:

$$\phi_k = (k-1)\frac{\pi}{M} \qquad \text{with } k = 1, \ldots, M \tag{5}$$

Considering the angle displacement given by (5), the k-th power cell output voltage can be re-written as:

$$v_k(t) = V_{dc,k} D_k + \sum_{n=1}^{\infty} \Big[a_{nk} \cos(n\omega t - n\phi_k) \Big] \tag{6}$$

According to the linearity property of the Fourier expansion series, the total CHB output voltage can be directly calculated as the sum of the output voltages of the M power cells, i.e:

$$\begin{aligned} v(t) &= \sum_{k=1}^{M} v_k(t) \\ &= \sum_{k=1}^{M} \Big[V_{dc,k} D_k + \sum_{n=1}^{\infty} \left[a_{nk} \cos(n\omega t - n\phi_k) \right] \Big] \end{aligned} \tag{7}$$

From (7), the n-th order harmonic content of the total CHB output voltage can be described by:

$$v\rfloor_n(t) = \sum_{k=1}^{M} a_{nk} \cos(n\omega t - n\phi_k), \tag{8}$$

Finally, applying the well-known cosine sum trigonometric formula $\cos(a \pm b) = \cos(a)\cos(b) \mp \sin(a)\sin(b)$ to decouple the Fourier harmonic coefficients from the carrier terms, (8) can be rewritten as:

$$\begin{aligned} v\rfloor_n(t) = \cos(n\omega t) &\sum_{k=1}^{M} \Big[a_{nk} \cos(n\phi_k) \Big] \\ + \sin(n\omega t) &\sum_{k=1}^{M} \Big[a_{nk} \sin(n\phi_k) \Big]. \end{aligned} \tag{9}$$

IV. Variable Angle PS-PWM Technique

In order to eliminate the n-th order harmonic distortion of the CHB output voltage, it is necessary to make zero the expressions inside square brackets in (9). If first harmonic order is considered ($n = 1$ which means $2f_c$ component) in a CHB with three cells ($M = 3$), it is necessary to solve the following system of equations in order to eliminate it:

$$\begin{aligned} a_{11} + a_{12}\cos(\phi_2) + a_{13}\cos(\phi_3) &= 0 \\ a_{12}\sin(\phi_2) + a_{13}\sin(\phi_3) &= 0 \end{aligned} \tag{10}$$

where ϕ_1 was considered $0°$ for convenience.

The solution to these equations is given by

$$\begin{aligned} \phi_2 &= \arccos\left(\frac{-a_{11}^2 - a_{12}^2 + a_{13}^2}{2a_{11}a_{12}}\right) \\ \phi_3 &= \arccos\left(\frac{-a_{11}^2 + a_{12}^2 - a_{13}^2}{2a_{11}a_{13}}\right) \end{aligned} \tag{11}$$

If the CHB is working under balanced conditions (same dc voltage for all the power cells $V_{dc,k} = V_{dc}$ and same duty cycle $D_k = D$), all Fourier coefficients a_{nk} are equal ($a_{nk} = a_n$). Applying these conditions in (11), the calculation of the phase displacement angles is simplified leading to

$$\begin{aligned} \phi_2 &= \arccos\left(-\frac{1}{2}\right) \rightarrow \phi_2 = 120°, 240° \\ \phi_3 &= \arccos\left(-\frac{1}{2}\right) \rightarrow \phi_3 = 240°, 120° \end{aligned} \tag{12}$$

These values of ϕ_k are those used in the conventional PS-PWM method. If these angles are considered, substituting them in (9) for the second harmonic, it can be demonstrated that $v\rfloor_2$=0. This result was expected because in the definition of the conventional PS-PWM method it is said that all harmonic distortion is zero up to $2Mf_c$ component (which coincides with $v\rfloor_3$).

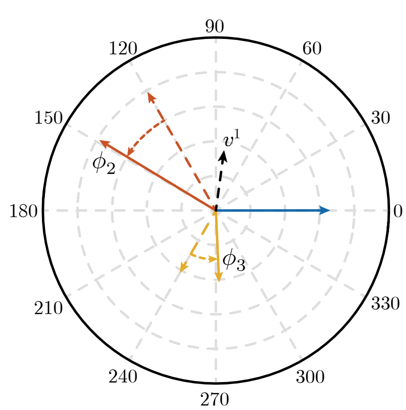

Fig. 6: Representation of the output voltages of the CHB cells and the corresponding harmonic content of the CHB output voltage at $2f_c$. Traditional angles in dashed lines and modified angles in solid lines.

However when the CHB is working under unbalanced conditions, each coefficient a_{nk} is different. In this case, if the conventional values of ϕ_k calculated in (12) are applied, $v\rfloor_1$ and $v\rfloor_2$ are not zero in general. So, the idea of the variable-angle PS-PWM method is to calculate the phase displacement angles needed to be applied depending on the instantaneous operational power converter conditions. Each sampling period, the a_{1k} coefficients have to be determined using (3), and finally the angles to be applied are calculated using (11).

TABLE I: Example of unbalanced operation point for a three-cell CHB.

H-Bridge parameter	1	2	3
$V_{dc,k}$ $[V]$	90	80	85
m_k	0.75	0.60	0.85

As an example, in Table I is presented a possible unbalanced operation point for a three-cell CHB power converter. Assuming this scenario, the vector system that describes this situation (during one sampling time) has been drawn in Fig. 6. As observed, the resulting fundamental harmonic $v\rfloor_1$ is different to zero when the conventional PS-PWM method is applied. However, using (11) it is possible to calculate new phase displacements angles to be applied in the PS-PWM method in order to cancel $v\rfloor_1$. The new angle disposition that removes this harmonic component is drawn using solid vectors in Fig. 6.

On the other hand, it can be affirmed that the valid solutions for the displacement angles ϕ_2 and ϕ_3 can be obtained only if the following conditions are met:

$$\begin{aligned} |a_{11} - a_{12}| \leq a_{13} \leq (a_{11} + a_{12}) \\ |a_{11} - a_{13}| \leq a_{12} \leq (a_{11} + a_{13}) \end{aligned} \tag{13}$$

In addition, according to (11), if some a_{1k} coefficient is equal to zero, the proposed variable angle technique does not present solution because of division by zero is not defined. In this way, the three-cell PS-PWM angle set must be fixed following the rule:

$$\begin{aligned} &\text{if } a_{11} = 0 \rightarrow [\phi_1, \phi_2, \phi_3] = [0, 0, 180]° \\ &\text{if } a_{12} = 0 \rightarrow [\phi_1, \phi_2, \phi_3] = [0, 0, 180]° \\ &\text{if } a_{13} = 0 \rightarrow [\phi_1, \phi_2, \phi_3] = [0, 180, 0]° \end{aligned} \tag{14}$$

During the CHB operation, each sampling time the outer control loop provides the reference voltage v^* to be generated by the CHB in order to achieve some specific control target. This reference voltage is conventionally shared equally by all power cells, achieving an inherent power equalization between the cells. So, the k-th reference voltage v_k^* is determined by

$$v_k^* = \frac{v^*}{M} \tag{15}$$

However, as was commented in section II, this conventional operation of the CHB can be changed in order to manage the power cell aging by modifying slightly the modulation index of each cell. This can be done including the weighting factor λ_k leading to

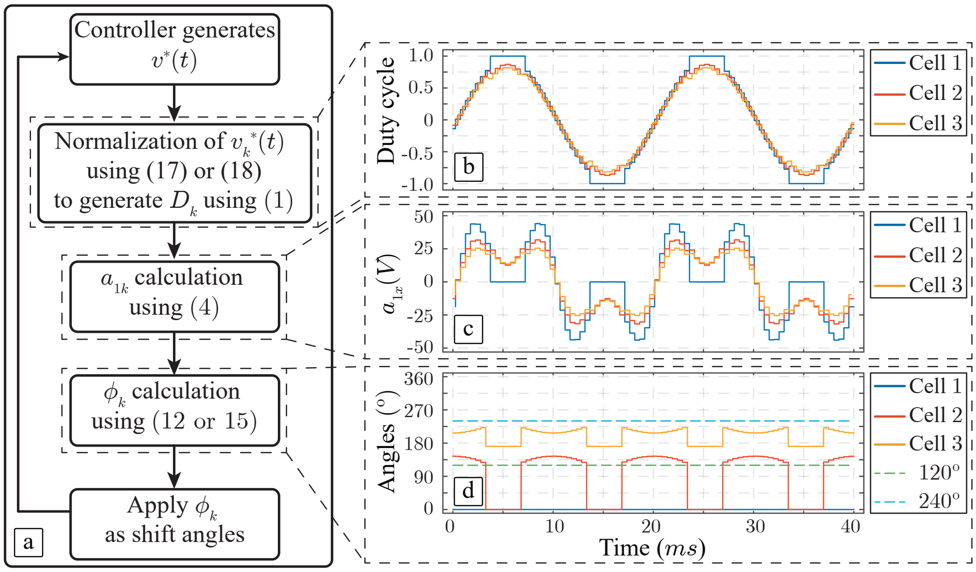

Fig. 7: Variable-angle flowchart application example for two complete grid periods. a) Linear flowchart. b) Duty cycle generation c) First harmonic content. d)Variable angle disposition.

$$v_k^* = \lambda_k \frac{v^*}{M} \qquad \text{where} \sum_{k=1}^{M} \lambda_k = M \tag{16}$$

Each cell reference voltage v_k^* is normalized respect to its corresponding dc voltage using (1), determining the duty cycle D_k represented in Fig. 7b. In addition, the n-th harmonic content of v_k^* is determined by (3). Applying this, the first harmonic content of k-th power cell (a_{1k}) is also drawn in Fig. 7c. Finally, according to the instantaneous operational conditions of the CHB and using (11), the angles to be applied in each power cell are obtained (see Fig. 7d where the conventional PS-PWM angles are also drawn in dashed lines).

As shown in Fig. 7b, a clamping period for the first power cell equal to 60° is applied. It has to be noticed that during the time where this cell is clamped, this specific cell reference voltage is saturated to the maximum value (positive or negative) and therefore the remaining power cells are forced to reduce their instantaneous duty cycles accordingly to achieve the same total reference voltage v^*. So, during this time, expression (15) is not fulfilled and the cell reference voltages are determined using

$$\begin{aligned} v_1^* &= \pm V_{dc,1} \\ v_k^* &= \frac{v^* \mp v_1^*}{M-1} \lambda_k \qquad \text{with } k = 2, \ldots, M \end{aligned} \tag{17}$$

This effect can be observed in Fig. 7b twice per cycle. Applying a duty cycle D_1 equal to ± 1 in (3), the resulting harmonic content a_{11} is equal to zero as it is shown in Fig. 7c. The angles calculation using (11) cannot be used in this case since the resulting angles would be undetermined. As a consequence, the angles are calculated using (14).

As a summary, in Fig. 7a the algorithm to implement the proposed variable-angle modulation technique in a control platform is presented. This flowchart has been implemented by simulation using a three-cell CHB power converter working under the unbalanced operation point presented in Table I. This routine must be run every sampling period because the phase displacement angles ϕ_k depend on the instantaneous values of duty cycles D_k and the dc voltages $V_{dc,k}$.

It is important to notice that the presented method is focused on a three-cell CHB but it can be extended for a CHB with a larger number of cells. However, the complexity of the corresponding equations to be solved, similar to those introduced in (10), increases as the number of cells grows. An initial approach to face this problem has been presented in [36].

V. Experimental Results

In order to validate the good performance, the proposed strategy has been tested in the laboratory prototype shown in Fig. 8. Each H-bridge is composed by four IXYB82N120C3H1 IGBTs from IXYS and the three-cell CHB converter is operated by the MPC5643L dual core 32-bit microprocessor from Freescale Semiconductor [37], [38]. The case temperature of one IGBT in each cell (S_{x1} in Fig. 1) is measured using fiber optics sensors (OTG-F) with a signal conditioner ProSens [39]. The temperature achieved by each IGBT inside cell will be approximately the same because the cell is modulated by unipolar PWM. The most important parameters and passive elements used in the experiment setup are summarized in Table II. To fix the voltage of the power cells, independent dc power supplies are used.

Three different scenarios (denoted as I, II and II) have been also tested and summarized in Table III. All experiments consider the CHB operating an ATC method with one clamped cell applying D-PWM (clamping angle equal to 60°) following the next structure: in the first 100 ms the behavior of the CHB using the traditional PS-PWM modulation technique is shown,

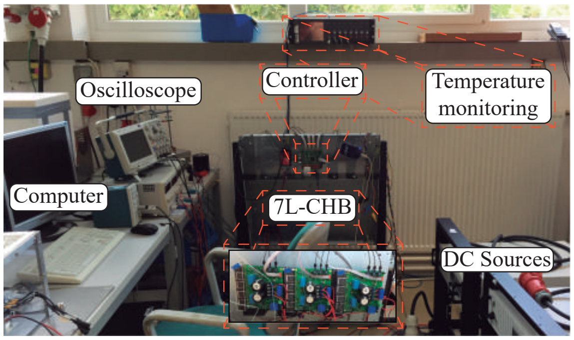

Fig. 8: Experimental setup composed by a three-cell CHB power converter, temperature datalogger and dc sources.

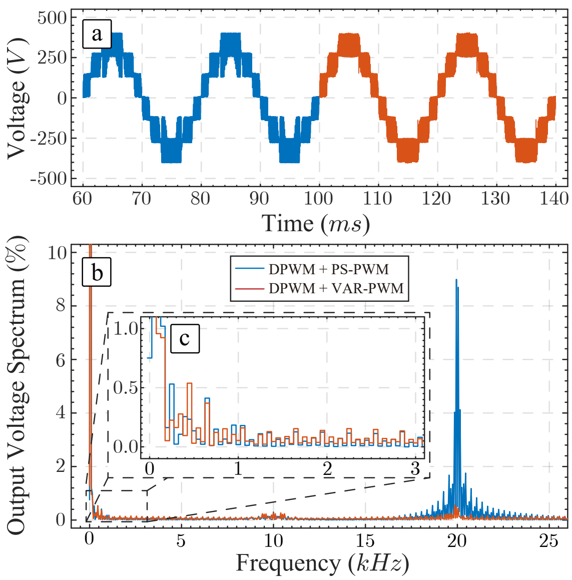

Fig. 9: Experimental result for operation point proposed by experiment I in Table III. PS-PWM is drawn in blue and variable-angle is plotted in red. a) CHB output voltage b) Harmonic spectrum c) Detail of the spectrum

using the blue color. After that, the proposed variable-angle modulation takes the control of the CHB operation and the results are drawn using red color.

Experiment I studies the behavior of the CHB converter when the operation point has different dc voltages and equal modulation indexes. Associated experimental results are shown in Fig. 9.

Experiment II proposes equal dc voltages but different

TABLE II: CHB parameters setup, passive elements and unbalanced operation point considered for the experiment.

Parameter	Value
Number of cells in the CHB	3
Cell switching frequency f_c (kHz)	10
Cell capacitance (mF)	2.2
Clamping angle ϕ_c $(°)$	60
Load Inductance (mH)	0.3
Load Resistance (Ω)	10

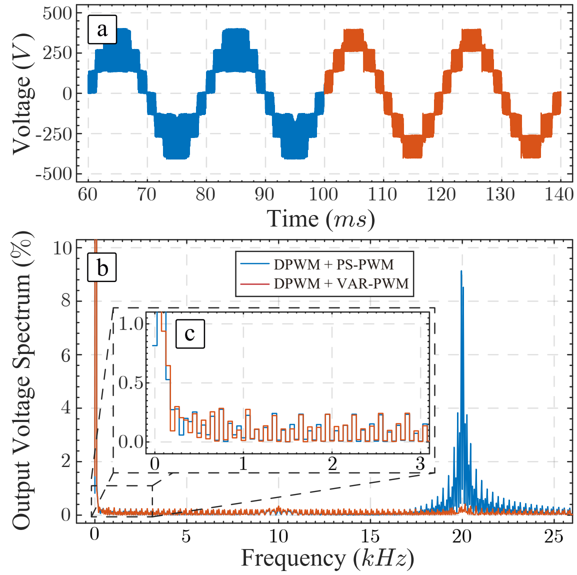

Fig. 10: Experimental result for operation point proposed by experiment II in Table III. PS-PWM is drawn in blue and variable-angle is plotted in red. a) CHB output voltage b) Harmonic spectrum c) Detail of the spectrum

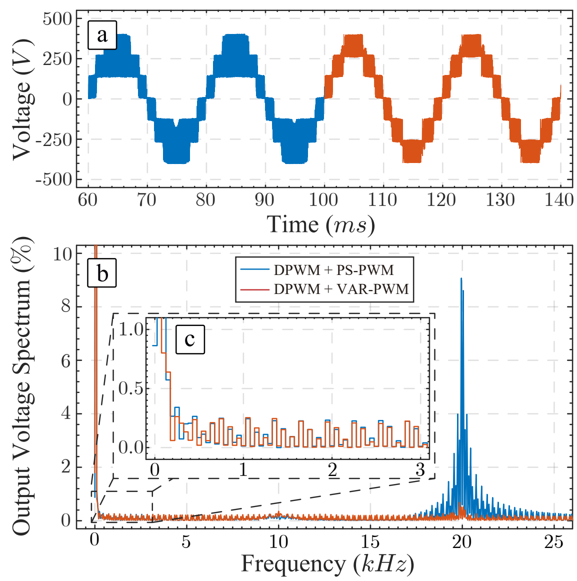

Fig. 11: Experimental result for operation point proposed by experiment III in Table III. PS-PWM is drawn in blue and variable-angle is plotted in red. a) CHB output voltage b) Harmonic spectrum c) Detail of the spectrum

modulation indexes. The harmonic spectrum of the output voltage is presented in Fig. 10.

Finally, experiment III is devoted to study the behavior of the CHB converter in a totally unbalanced operation, that is, different dc voltages and modulation indexes. The output voltage harmonic spectrum can be consulted in Fig. 11.

All experiments have in common the high output voltage distortion located at $2f_c$ when the PS-PWM modulation is used in combination with D-PWM technique. It is clear that the harmonic distortion as well as the typical base-bands present at

TABLE III: Proposed experimental setup scenarios

Experiment	DC Voltage $[V]$	Duty Cycles
I	$[125, 135, 145]$	$[0.8, 0.8, 0.8]$
II	$[135, 135, 135]$	$[0.5, 0.9, 1.0]$
III	$[134, 130, 140]$	$[0.5, 0.9, 1.0]$

$2f_c$ are completely removed (or massively reduced, depending on the case) when the variable-angle technique is applied. Moreover, a zoomed version of the low-order components of the output voltage spectrum is also provided. As it is highlighted in Fig. 9c, Fig. 10c and Fig. 11c, the variable-angle technique does not affect negatively to the low-order components. This fact can be consulted in Table IV where the THD as well as the weighted THD (WTHD) values have been experimentally measured up to 50-th harmonic order.

TABLE IV: THD and WTHD considering up to 50-th harmonic order extracted from experimental results

	PS-PWM		Variable-angle PS-PWM	
Experiment	THD [%]	WTHD [%]	THD[%]	WTHD[%]
I	1.826	0.701	1.629	0.578
II	1.670	0.663	1.482	0.523
III	1.637	0.632	1.360	0.462

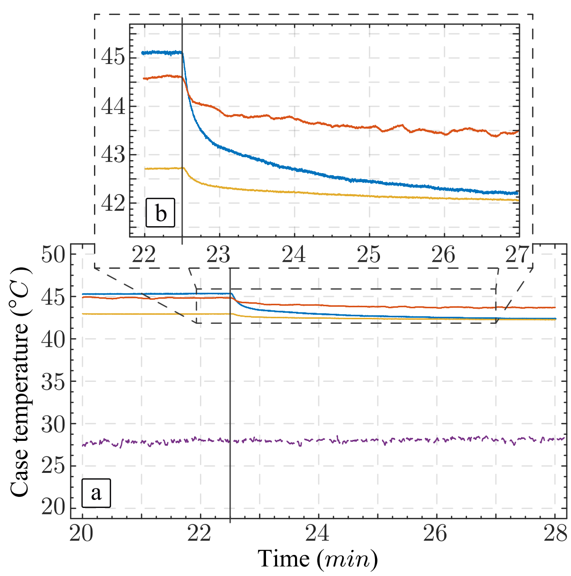

Fig. 12: Thermal experimental results for experiment III in Table III. IGBT case temperature in each power cell. The color scheme is as follows: first cell is drawn in blue, red is used for second cell and third cell is plotted in yellow. Ambient temperature is purple

Finally, it is necessary to validate the CHB thermal behavior. In this way, in Fig. 12 the device case temperature of each cell is shown when the proposed strategy is used. The experiment is carried out under a constant ambient temperature equal to $28°C$. Until $t = 22.5$ minutes, the CHB is conventionally operated using PS-PWM considering the operation point proposed in experiment III. In this scenario, the power cells reach case temperatures equal to 45.1, 44.6 and $42.7°C$, respectively. It has to be noticed that all power devices in one cell achieve the same case temperature due to the symmetric operation of the unipolar PWM method.

After $t = 22.5$ minutes of operation, the D-PWM based ATC method (clamping angle equal to $60°$) with variable-angle PS-PWM is activated leading to a significant temperature reduction as observed in Fig. 12. It demonstrates the effectiveness of the D-PWM with variable-angle PS-PWM method to achieve the active thermal control. Taking the experimental results into account, it can be affirmed that the reliability function introduced in [40] will be improved because using the clamped-cell based ATC method the obtained power losses are reduced. Finally, it can be noticed that from a superior level, an operation & maintenance system will manage the power converter determining every sampling period the value of the clamping angle in order to optimize the operation & maintenance system costs. At first sight, the balance of the aging mismatch could be a proper target but other options could be also attractive taking into account other issues as pre-programmed system maintenance or potential fault tolerant capability features.

VI. Conclusions

Reducing as much as possible the maintenance costs is a key factor of commercial power converters. Prognostic maintenance should be implemented in order to improve the power converter availability. In a modular structure such as the CHB, the possibility to delay the failure of one cell by means of active thermal control could allow to implement planned maintenance. Unfortunately, the active thermal control methods applied to CHB usually introduce harmonic distortion at low frequency which is a drawback in terms of output waveforms degraded quality and corresponding extra filtering costs.

In this paper, the active thermal control method based on modifying the modulation indexes of the power cells including a discontinuous PWM technique for one cell is used. In order to avoid the disadvantages of this active thermal control method, a modification of the conventional PS-PWM technique is applied. The proposed method is a variable angle PS-PWM where the phase displacement angles between consecutive power cells are not fixed. The calculation of the phase displacement angles to be applied is based on the Fourier analysis of the power cell waveforms. The required calculations are computationally simple and are carried out every sampling time.

Experimental results are included in the paper in order to validate the proposed method. It is demonstrated that the thermal control of the CHB topology is correctly applied while the low-order harmonic distortion located at twice the carrier frequency is eliminated. The experimental results show how the proposed strategy improves the harmonic spectrum of the output waveforms without affecting the thermal control.

REFERENCES

[1] A. Nabae, I. Takahashi, and H. Akagi, "A new neutral-point-clamped pwm inverter," *IEEE Transactions on Industry Applications*, vol. IA-17, no. 5, pp. 518–523, Sept 1981.

[2] S. Kouro, M. Malinowski, K. Gopakumar, J. Pou, L. G. Franquelo, B. Wu, J. Rodriguez, M. A. Perez, and J. I. Leon, "Recent advances and industrial applications of multilevel converters," *IEEE Transactions on Industrial Electronics*, vol. 57, no. 8, pp. 2553–2580, Aug 2010.

[3] M. Malinowski, K. Gopakumar, J. Rodriguez, and M. A. Perez, "A survey on cascaded multilevel inverters," *IEEE Transactions on Industrial Electronics*, vol. 57, no. 7, pp. 2197–2206, July 2010.

[4] W. Mcmurray, "Fast response stepped-wave switching power converter circuit," May 25 1971, uS Patent 3,581,212. [Online]. Available: https://www.google.com/patents/US3581212

[5] P. Kakosimos and H. Abu-Rub, "Predictive control of a grid-tied cascaded full-bridge npc inverter for reducing high-frequency common-mode voltage components," *IEEE Transactions on Industrial Informatics*, vol. 14, no. 6, pp. 2385–2394, June 2018.

[6] M. Liserre, G. Buticchi, M. Andresen, G. D. Carne, L. F. Costa, and Z. X. Zou, "The smart transformer: Impact on the electric grid and technology challenges," *IEEE Industrial Electronics Magazine*, vol. 10, no. 2, pp. 46–58, June 2016.

[7] L. F. Costa, G. D. Carne, G. Buticchi, and M. Liserre, "The smart transformer: A solid-state transformer tailored to provide ancillary services to the distribution grid," *IEEE Power Electronics Magazine*, vol. 4, no. 2, pp. 56–67, June 2017.

[8] J. I. Leon, S. Vazquez, and L. G. Franquelo, "Multilevel converters: Control and modulation techniques for their operation and industrial applications," *Proceedings of the IEEE*, vol. 105, no. 11, pp. 2066–2081, Nov 2017.

[9] J. Napoles, A. J. Watson, J. J. Padilla, J. I. Leon, L. G. Franquelo, P. W. Wheeler, and M. A. Aguirre, "Selective harmonic mitigation technique for cascaded h-bridge converters with nonequal dc link voltages," *IEEE Transactions on Industrial Electronics*, vol. 60, no. 5, pp. 1963–1971, May 2013.

[10] J. I. Leon, S. Kouro, L. G. Franquelo, J. Rodriguez, and B. Wu, "The essential role and the continuous evolution of modulation techniques for voltage-source inverters in the past, present, and future power electronics," *IEEE Transactions on Industrial Electronics*, vol. 63, no. 5, pp. 2688–2701, May 2016.

[11] D. G. Holmes and T. A. Lipo, *CarrierBased PWM of Multilevel Inverters*. IEEE, 2003. [Online]. Available: https://ieeexplore.ieee.org/xpl/articleDetails.jsp?arnumber=5311978

[12] B. Wu and M. Narimani, *Cascaded H-Bridge Multilevel Inverters*. Wiley-IEEE Press, 2017, pp. 480–. [Online]. Available: http://ieeexplore.ieee.org/xpl/articleDetails.jsp?arnumber=7827420

[13] M. Held, P. Jacob, G. Nicoletti, P. Scacco, and M. H. Poech, "Fast power cycling test of igbt modules in traction application," in *Proceedings of Second International Conference on Power Electronics and Drive Systems*, vol. 1, May 1997, pp. 425–430 vol.1.

[14] H. Huang and P. A. Mawby, "A lifetime estimation technique for voltage source inverters," *IEEE Transactions on Power Electronics*, vol. 28, no. 8, pp. 4113–4119, Aug 2013.

[15] M. Andresen, K. Ma, G. Buticchi, J. Falck, F. Blaabjerg, and M. Liserre, "Junction temperature control for more reliable power electronics," *IEEE Transactions on Power Electronics*, vol. 33, no. 1, pp. 765–776, Jan 2018.

[16] H. Lu, T. Tilford, C. Bailey, and D. R. Newcombe, "Lifetime prediction for power electronics module substrate mount-down solder interconnect," in *2007 International Symposium on High Density packaging and Microsystem Integration*, June 2007, pp. 1–10.

[17] I. F. Kovacevic, U. Drofenik, and J. W. Kolar, "New physical model for lifetime estimation of power modules," in *The 2010 International Power Electronics Conference - ECCE ASIA -*, June 2010, pp. 2106–2114.

[18] H. Salimian and H. Iman-Eini, "Fault-tolerant operation of three-phase cascaded h-bridge converters using an auxiliary module," *IEEE Transactions on Industrial Electronics*, vol. 64, no. 2, pp. 1018–1027, Feb 2017.

[19] M. Liserre, M. Andresen, L. Costa, and G. Buticchi, "Power routing in modular smart transformers: Active thermal control through uneven loading of cells," *IEEE Industrial Electronics Magazine*, vol. 10, no. 3, pp. 43–53, Sept 2016.

[20] C. H. van der Broeck, L. A. Ruppert, R. D. Lorenz, and R. W. D. Doncker, "Methodology for active thermal cycle reduction of power electronic modules," *IEEE Transactions on Power Electronics*, pp. 1–1, 2018.

[21] Wintrich, U. Nicolai, W. Tursky, and T. Reimann, "Semikron application manual power semiconductors," 2011.

[22] Y. Ko, M. Andresen, G. Buticchi, and M. Liserre, "Power routing for cascaded h-bridge converters," *IEEE Transactions on Power Electronics*, vol. 32, no. 12, pp. 9435–9446, Dec 2017.

[23] ——, "Thermally compensated discontinuous modulation strategy for cascaded h-bridge converters," *IEEE Transactions on Power Electronics*, vol. 33, no. 3, pp. 2704–2713, March 2018.

[24] V. G. Monopoli, Y. Ko, G. Buticchi, and M. Liserre, "Performance comparison of variable-angle phase-shifting carrier pwm techniques," *IEEE Transactions on Industrial Electronics*, vol. 65, no. 7, pp. 5272–5281, July 2018.

[25] S. Kouro, P. Lezana, M. Angulo, and J. Rodriguez, "Multicarrier pwm with dc-link ripple feedforward compensation for multilevel inverters," *IEEE Transactions on Power Electronics*, vol. 23, no. 1, pp. 52–59, Jan 2008.

[26] Y. Cho, T. LaBella, J. Lai, and M. K. Senesky, "A carrier-based neutral voltage modulation strategy for multilevel cascaded inverters under unbalanced dc sources," *IEEE Transactions on Industrial Electronics*, vol. 61, no. 2, pp. 625–636, Feb 2014.

[27] J. Pou, D. Boroyevich, and R. Pindado, "New feedforward space-vector pwm method to obtain balanced ac output voltages in a three-level neutral-point-clamped converter," *IEEE Transactions on Industrial Electronics*, vol. 49, no. 5, pp. 1026–1034, Oct 2002.

[28] J. I. Leon, S. Vazquez, A. J. Watson, L. G. Franquelo, P. W. Wheeler, and J. M. Carrasco, "Feed-forward space vector modulation for single-phase multilevel cascaded converters with any dc voltage ratio," *IEEE Transactions on Industrial Electronics*, vol. 56, no. 2, pp. 315–325, Feb 2009.

[29] S. Lu, S. Mariéthoz, and K. A. Corzine, "Asymmetrical cascade multilevel converters with noninteger or dynamically changing dc voltage ratios: Concepts and modulation techniques," *IEEE Transactions on Industrial Electronics*, vol. 57, no. 7, pp. 2411–2418, July 2010.

[30] M. Liserre, V. G. Monopoli, A. Dell'Aquila, A. Pigazo, and V. Moreno, "Multilevel phase-shifting carrier pwm technique in case of non-equal dc-link voltages," in *IECON 2006 - 32nd Annual Conference on IEEE Industrial Electronics*, Nov 2006, pp. 1639–1642.

[31] S. Li, Z. Yang, Q. Li, J. Gong, J. Sun, and X. Zha, "Asymmetrical phase-shifting carrier pulse-width modulation for harmonics suppression in cascaded multilevel converter under unbalanced dc-link voltages," in *2015 IEEE Energy Conversion Congress and Exposition (ECCE)*, Sept 2015, pp. 6804–6810.

[32] Y. Sun, J. Zhao, and Z. Ji, "An improved cps-pwm method for cascaded multilevel statcom under unequal losses," in *IECON 2013 - 39th Annual Conference of the IEEE Industrial Electronics Society*, Nov 2013, pp. 418–423.

[33] A. Marquez, J. I. Leon, S. Vazquez, R. Portillo, L. G. Franquelo, E. Freire, and S. Kouro, "Variable-angle phase-shifted pwm for multilevel three-cell cascaded h-bridge converters," *IEEE Transactions on Industrial Electronics*, vol. 64, no. 5, pp. 3619–3628, May 2017.

[34] V. G. Monopoli, A. Marquez, J. I. Leon, Y. Ko, G. Buticchi, and M. Liserre, "Improved harmonic performance of cascaded h-bridge converters with thermal control," *IEEE Transactions on Industrial Electronics*, pp. 1–1, 2018.

[35] H. S. H. S. Carslaw, "Introduction to the theory of fourier's series and integrals," New York, 1950.

[36] A. Marquez, J. I. Leon, S. Vazquez, L. G. Franquelo, and S. Kouro, "Adaptive phase-shifted pwm for multilevel cascaded h-bridge converters with large number of power cells," in *2017 11th IEEE International Conference on Compatibility, Power Electronics and Power Engineering (CPE-POWERENG)*, April 2017, pp. 430–435.

[37] Ixysb82n120c3h1 igbt datasheet. [Online]. Available: http://www.ixys.com/

[38] Mpc5643l micro controller datasheet. [Online]. Available: https://www.nxp.com/docs/en/data-sheet/MPC5643L.pdf

[39] Opsens solutions. [Online]. Available: https://opsens-solutions.com/

[40] M. M. Haji-Esmaeili, M. Naseri, H. Khoun-Jahan, and M. Abapour, "Fault-tolerant structure for cascaded h-bridge multilevel inverter and reliability evaluation," *IET Power Electronics*, vol. 10, no. 1, pp. 59–70, 2017.

Abraham Marquez (S'14-M'16) was born in Huelva, Spain, in 1985. He received his B.S. and M.S. degrees in telecommunications engineering in 2014 and 2016 from the Universidad de Sevilla (US), Spain, where he is currently working toward the PhD degree in electronic engineering.

His main research interest are modulation techniques, multilevel converters, power conversion for renewable energy sources and model-based predictive control of power converters and drives. Mr. Marquez was recipient as coauthor of the 2015 Best Paper Award of the IEEE Industrial Electronics Magazine.

Vito Giuseppe Monopoli (S'98-M'05-SM'18) received the M.S. and PhD degrees in electrical engineering from the Bari Polytechnic, in 2000 and 2004, respectively. He is currently an Assistant Professor Bari Polytechnic, Bari, Italy.

His research activity concerns multilevel converters and the analysis of harmonic distortion produced by power converters and electrical drives. He is particularly interested in innovative control techniques for power converters. He is member of the IEEE Industry Applications Society, IEEE Industrial Electronics Society and IEEE Power Electronics Society.

Jose I. Leon (S'04-M'07-SM'14-F'17) was born in Cadiz, Spain. He received the B.S., M.S., and PhD degrees in telecommunications engineering from Universidad de Sevilla (US), Seville, Spain, in 1999, 2001, and 2006, respectively. Currently, he is an Associate Professor with the Department of Electronic Engineering, US.

His research interests include modulation and control of power converters for high-power applications and renewable energy systems. He is currently serving as an Associate Editor of the IEEE Transactions on Industrial Electronics. Dr. Leon was a co-recipient of the 2008 and 2015 Best Paper Award of IEEE Industrial Electronics Magazine and the 2012 Best Paper Award of the IEEE Transactions on Industrial Electronics. He was the recipient of the 2014 IEEE J. David Irwin Industrial Electronics Society Early Career Award, the 2017 IEEE Bimal K. Bose Energy Systems Award and the 2017 Manuel Losada Villasante Award for excellence in research and innovation. In 2017 he has been elevated to the IEEE fellow grade with the following citation "for contributions to high-power electronic converters".

Youngjong Ko (S'16) received his B.S. and M.S. degrees in Electronic Engineering from the Ajou University, Suwon, Korea in 2009 and 2012, respectively. Since 2015 he is working toward his Ph.D degree from the chair of power electronics at the Kiel University, Germany.

His research interests include grid-connected power converter and reliability in power electronics.

Giampaolo Buticchi (S'10-M'13-SM'17) received the Master degree in Electronic Engineering in 2009 and the PhD degree in Information Technologies in 2013 from the University of Parma, Italy. In 2012 he was visiting researcher at The University of Nottingham, UK. Between 2014 and 2017 he was a post-doctoral researcher at the University of Kiel, Germany. He is now Associate Professor in Electrical Engineering at The University of Nottingham Ningbo China.

His research focuses on power electronics for renewable energy systems, smart transformer fed micro-grids and dc grids for the More Electric Aircraft. He is author/co-author of more than 160 scientific papers.

Sergio Vazquez (S'04-M'08-SM'14) was born in Seville, Spain, in 1974. He received the M.S. and PhD degrees in industrial engineering from the University of Seville (US) in 2006, and 2010, respectively.

Since 2002, he is with the Power Electronics Group working in R&D projects. He is an Associate Professor with the Department of Electronic Engineering, US. His research interests include power electronics systems, modeling, modulation and control of power electronics converters applied to renewable energy technologies.

Dr. Vazquez was recipient as coauthor of the 2012 Best Paper Award of the IEEE Transactions on Industrial Electronics and 2015 Best Paper Award of the IEEE Industrial Electronics Magazine. He is involved in the Energy Storage Technical Committee of the IEEE industrial electronics society and is currently serving as an Associate Editor of the IEEE Transactions on Industrial Electronics.

Marco Liserre (S'00-M'02-SM'07-F'13) received the M.S. and PhD degree in Electrical Engineering from the Bari Polytechnic, respectively in 1998 and 2002. He has been Associate Professor at Bari Polytechnic and from 2012 Professor in reliable power electronics at Aalborg University (Denmark). From 2013 he is Full Professor and he holds the Chair of Power Electronics at Kiel University (Germany). He has published over 350 technical papers and a book. receiving more than 25000 citations. Marco Liserre is listed in ISI Thomson report "The world's most influential scientific minds" from 2014.

He has been awarded with an ERC Consolidator Grant for the project "The Highly Efficient And Reliable smart Transformer (HEART), a new Heart for the Electric Distribution System" and with the ERC Proof of Concept Grant U-HEART.

He is member of IAS, PELS, PES and IES. He has received the IES 2009 Early Career Award, the IES 2011 Anthony J. Hornfeck Service Award, the 2014 Dr. Bimal Bose Energy Systems Award, the 2011 Industrial Electronics Magazine best paper award the Third Prize paper award by the Industrial Power Converter Committee at ECCE 2012, 2012, the 2017 IEEE PELS Sustainable Energy Systems Technical Achievement Award and the 2018 IEEE IES Mittelmann Achievement Award which is the highest award of the IEEE-IES.

Leopoldo G. Franquelo (M'84-SM'96-F'05) received the M.Sc. and Ph.D. degrees in electrical engineering from the Universidad de Sevilla, Spain, in 1977 and 1980, where he was associate professor from 1982-86 and is full professor since 1986. Also, he is a 1000 Talent Professor at the Department of Control Science and Engineering in Harbin Institute of Technology (China) since 2016.

His current research interests include modulation techniques for multilevel inverters and power electronic systems for renewable energy systems. He has participated in more than 100 Industrial and $R\&D$ projects and has published more than 300 papers, 76 of them in IEEE Journals. Dr. Franquelo is an Industrial Electronics Society Distinguished Lecturer since 2006. In the IEEE Trans. on Ind. Electronics, he became an Associate Editor in 2007, Co-EiC in 2014, and the EiC since 2016. He was a Member-at-Large of the IES AdCom (2002-2003) and Vice President for Conferences (2004-2007). He was the President of the IES (2010-2011) and is an IES AdCom Life member. In 2009 and 2013, he received the Andalusian Research Award and FAMA Award recognizing the excellence of his research career. He has received a number of Best Paper Awards from IEEE journals. He was the recipient of the Eugene Mittelmann Outstanding Research Achievement Award and the Antohny J. Hornfeck Service Award from IEEE-IES, in 2012 and 2015 respectively.